npj | heritage science

Article

https://doi.org/10.1038/s40494-025-02121-y

Baroque stucco techniques of Baldassarre Fontana at Kroměříž Château

Jan Válek[1], Sylwia Svorová Pawełkowicz[1], Petr Kozlovcev[1], Jana Zapletalová[2], Marta Caroselli[3] ✉, Dita Frankeová[1] & Kristýna Kotková[1]

This study investigates the materials and construction techniques employed in the Baroque stucco decorations of the ground-floor halls at Kroměříž Château, executed by Baldassarre Fontana and his workshop. The material composition of sixteen samples was analysed using optical microscopy, SEM-EDS, XRD, thermal analysis, and acid dissolution. The results revealed the deliberate use of high-purity calcitic lime, sourced from Devonian limestone near Přerov and gypsum from the Ketř-Opava basin. Two mortar types were identified: a lime-gypsum-sand core modelling mortar and a lime-rich finishing stucco mortar, reflecting layered application techniques. The presence of crushed marble in certain decorations suggests recipe changes and indicates a multi-phase construction process possibly extending beyond Fontana's supervision. Surface finishes were initially limited to white limewash, later overpainted with layers containing zinc white pigments. The findings highlight 17th-century stucco practices, provide a foundation for further conservation and historical research, and establish a benchmark for Central-European Baroque stucco studies.

Stucco decorations have been the subject of recent studies aiming to understand their composition, structure and the general technology of their production[1]. These analyses have provided interesting information regarding the composition, structure and the original recipes prompting further, more detailed research[2–5]. It has also been shown that material analysis is fundamental in guiding informed decision-making during restoration design[6]. These two directions currently represent the main motivation for further research: (i) to gain more detailed knowledge about a specific historical technique linked to a building, an artist or a period, or (ii) to provide technical information in order to ensure appropriate, knowledge-based preservation of stucco works. Both of these areas are based on material analyses, which can describe the composition and quality of the materials used, as well as provide information about the artistic technique itself.

Stucco is a decorative technique with roots in antiquity[7]. It is essentially plasterwork that decorates walls and ceilings with plastic low or high reliefs, or relief sculptures[8]. Studies have shown that Baroque stucco is usually executed as a layered mortar structure with a core made of lime, gypsum and sand covered by a lime-rich finishing mortar[5,6]. In some regions, the term stucco has also taken hold as a general term for a fine mortar with aggregates under one millimetre, which is used as the final layer on plaster or render.

Analytical methods used for historical mortars can also be applied to characterize stucco materials[9]. However, the description of the technique is more complex; material analysis only partially contributes to its understanding. It is possible to draw on historical treatises[10–13], but individual artists adapted their techniques based on available materials and empirical craft experience[2]. Therefore, treatises normally contain general instructions, while the actual practice depended on specific workshops in specific geographical conditions and the historical period during which the work was created. Understanding the technique is especially challenging because we are examining it from today's perspective. The technology and materials used to make these traditional decorations changed significantly over time, and what once required no explanation may now constitute vital missing information.

Kroměříž in Moravia was the seat of the bishops and archbishops of Olomouc in the early modern period. After the Thirty Years' War, Bishop Karl von Lichtenstein-Castelcorno initiated and oversaw the reconstruction of the monumental Archbishop's Château (UNESCO World Heritage Site) in its present form. The Château was built in 1688 according to the plans of the architect Giovanni Pietro Tencalla (1629-1702). The construction and decoration of the Château are well documented by numerous archival documents[14,15]. The studied stuccoes by Baldassarre Fontana are found in the ground-floor halls (terrene salons) of the Château, which represent the most authentically preserved early modern part of the decoration[16,17]. The halls, located in the basement of the north wing of the Château, consist of three rooms on the transverse axis of the wing, each side ending with a grotto, Fig. 1. Stucco decorates the vaults and walls of all three halls. In addition to B. Fontana, the painter Paolo Pagani (1655–1716) and the sculptor Fedele Raggi (c. 1637–1693) contributed to the decoration of the

[1]Institute of Theoretical and Applied Mechanics of the Czech Academy of Sciences, Prague, Czech Republic. [2]Palacký University Olomouc, Olomouc, Czech Republic. [3]University of Applied Arts and Sciences of Southern Switzerland (SUPSI), Mendrisio, Switzerland. ✉e-mail: Marta.Caroselli@supsi.ch

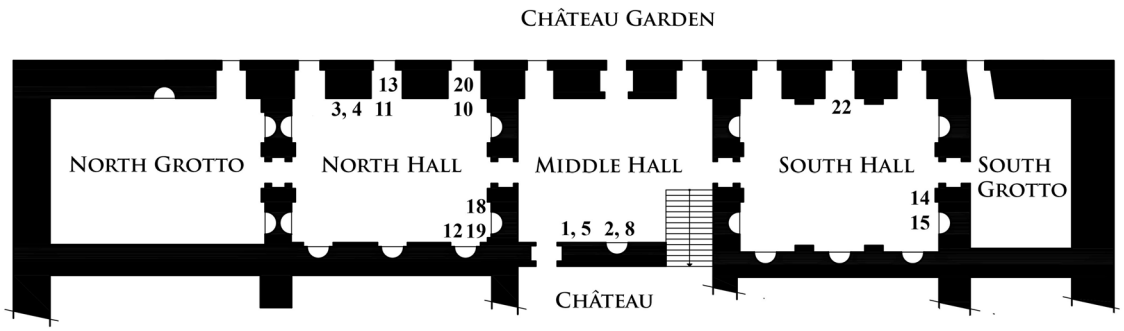

Fig. 1 | Schematic Layout. Arrangement of the ground floor halls and the sample positions.

Fig. 2 | South hall stuccoes. Location of samples at the back of the putto (**A**). Sample STK 14 of a core modelling mortar (**B**), and sample STK 15 of a stucco finishing layer (**C**) from a relief sculpture.

interiors. The stucco decorations by Fontana and his collaborators in the halls, created sometime between 1690 and 1693, are of exceptional artistic quality and are among the finest works of his career. Illusionistic effects are used prominently. The stuccoes depict figural motifs of large and small angels, as well as high-quality decorations of fruit and flower festoons, baskets with fruit and flowers, and trophies[17–19].

In the early modern period, artists and craftsmen from around Lake Lugano and the nearby territories of the present-day Italian–Swiss border region (Canton of Ticino and the Lombardy region) were particularly specialised in stucco decoration. These artists and craftsmen developed a distinctive type of migration that spanned the whole of Europe for several centuries (evidenced during the 15–18th centuries)[20–23]. Large teams of people composed of architects, masons, plasterers, sculptors, painters and other artisan professions, often closely connected by blood and neighbourhood ties, were able to realise the completion of entire buildings from plans to interior decoration in various parts of Europe. Plasterers held an important position within the system and possessed unique know-how. They were characterised by their extraordinary flexibility in adapting to local requirements and conditions, as well as the wishes of their clients, while achieving identical artistic effects using mostly local materials[4]. Surviving accounting documents and contracts suggest that they travelled light, perhaps only transporting drawings and graphic designs. A common arrangement was that heavier items and materials were provided locally by the commissioner.

A general picture of the available materials is known based on archival documents[14]. Lime was burnt in the Château's own limekilns. An older kiln, positioned nearby, was in operation up to around 1670–80, and the main raw material processed there was a silty limestone of Jurassic age. At the time when the studied stuccoes were produced (since 1688), a new limekiln was brought into operation in Chrášťany, approximately 8 km away from the Château, where, in addition to the silty limestone, Lower Devonian limestone from the vicinity of Přerov was also burnt. This fine-grained, bench-shaped limestone was generally more difficult to acquire but was preferred for its white colour and possibly other properties. In contrast, the silty Jurrasic limestone was known to produce a grey-ochre lime, noted for its hydraulic properties, especially when industrially produced at the end of 19th and in the first half of the 20th century. Gypsum was bought from Ketř in Kladsko (Opava Basin), which is about 130 km to the north, and this evaporitic deposit was in fact the only source of gypsum in the former Czech territory.

This analytical study was undertaken in order to improve the understanding of the stucco technology at the end of the 17th and the beginning of the 18th century, the high-baroque period in Central Europe. In addition, the study aimed to evaluate whether or not any specific material or technological imprints exist that can be linked to the craftsmen and workshops who carried out the work. For this reason, the study focused on one of the leading stucco-makers of the time, Baldassarre Fontana (1661–1733)[24–27] and on the work he produced in Kroměříž for a major patron, the bishop of Olomouc, Karl von Liechtenstein-Castelcorno (1624–1695), a notable supporter of high artistic quality. The study also addresses the question of how the travelling craftsmen adapted to the specific properties of locally available materials.

Methods

Samples

Samples were selected from positions where earlier damage has occurred, making it possible to assess the stratigraphy of the stucco layers. As the result of extreme damage, where part of the forearm of a putto was separated from the remaining torso due to corrosion of the internal supporting element, it was possible to study the construction of relief sculptures. The sampling positions were carefully documented and the selected areas are shown in Figs. 1–4. Three types of stucco decorations are represented in the sample

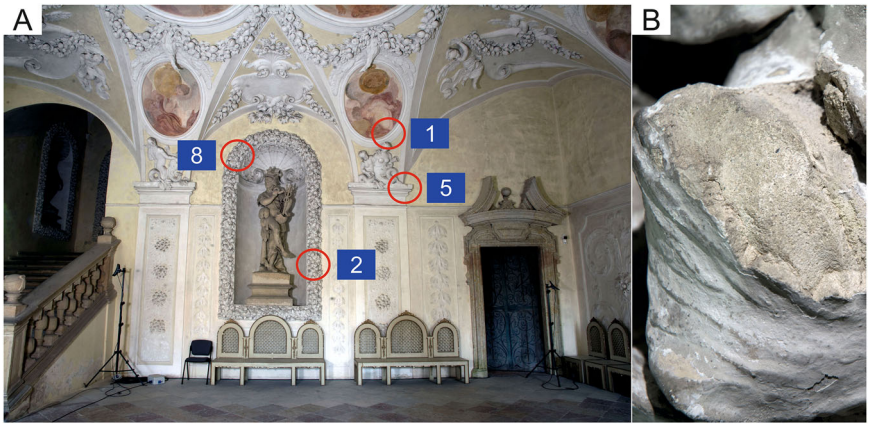

Fig. 3 | Middle hall stuccoes. Samples STK 2, 8 of a high-relief niche-frame decoration and samples STK 1, 5—hair and tail of a naiad. **A** Detail of sample STK 8—previously detached finishing stuccolayer exposing the core made of modelling mortar (**B**).

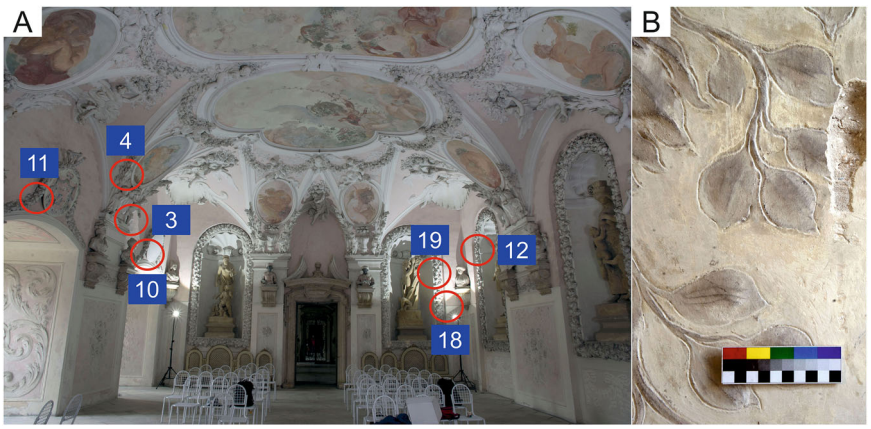

Fig. 4 | North hall stuccoes. Sample STK 3 from a relief sculpture, putto's forearm; sample STK 4—low relief behind the putto; samples STK 10, 11—garlands above the entrances; samples STK 12, 18, 19—niche frames decorations; STK 13, 20—wall decoration frames (**A**). Detail of the decoration panel, sample STK 20, on the side wall of one of the three entrances to the hall from the park (**B**).

set: stucco relief sculptures, high-relief garlands, and low-relief decorative panels on the walls, Table 1.

Analytical approach

The samples were documented macroscopically and their surface treatments were assessed using a stereomicroscope. The samples consisting of multiple layers were decomposed to their individual structural parts—typically to the finishing layer and the core mortar—and the separated samples were designated with additional letters A, B, and C. Subsequently, each sample was processed according to the proposed analytical objectives. Four samples were large enough to determine the soluble/insoluble ratio by acid dissolution. Special attention was paid to so-called binder related particles (BRPs); for their classification see ref.[28]. BRPs are lumps of binder of various sizes and structures that are rich in binder and contain no aggregate. Their origin depends on the technology used in the production and processing of the binder. Sampling was only possible in already damaged parts and thus, for example, no core modelling mortar was taken from the high-relief decorations of the niches.

The stucco mortar characteristics and composition were analysed in detail by means of polarised light microscopy (PLM) and scanning electron microscopy. For these microscopic observations, polished thin-sections and polished cross-sections were prepared. The thin-sections were studied in plane-polarised (PPL) and crossed-polarised transmitted light (XPL); polished sections were studied in reflected light (RL) and ultraviolet fluorescence (UV), using an Olympus BX53M microscope equipped with an Olympus DP27 digital camera.

Scanning electron microscopy (SEM) was performed using a Tescan MIRA II LMU instrument equipped with a Bruker AXS energy dispersive analytical system (EDS). The EDS measuring conditions were as follows: a carbon coated polished surface, accelerating voltage of electrons 15 kV, working distance (WD) of 15 mm, high vacuum. The images were taken with a back-scattered electron (BSE) detector. The sites where the elemental composition was determined were chosen with respect to the homogeneity of the measured areas. The chemical composition of the binder was used to determine its purity in terms of the content of its main compound, calcium carbonate. In addition, ratio of silica, alumina, and iron oxides to calcium and magnesium oxides, expressed as the cementation index (ci, Eq. (1)), was used to classify the binder as air lime (ci < 0.3) or feebly hydraulic lime (0.3 < ci < 0.5) following the system[29].

$$ci = \frac{2.8xSiO_2 + 1.1xAl_2O_3 + 0.7xFe_2O_3}{CaO + 1.4xMgO} \quad (1)$$

The composition of the binder component of the mortars was characterised by means of thermogravimetric analysis (TGA/DTG) and X-ray powder diffraction (XRD). Firstly, the coating layers were mechanically removed and the purged samples were gently crushed. The obtained material was passed through a 63 µm sieve. The fraction below 63 µm was used further for analyses. The TA Instruments SDT Q600 was used to measure thermal behaviour between 25 °C and 1000 °C for which a sample of approximately 10 mg was heated at the rate of 20 °C/min in nitrogen atmosphere with a flow rate at 100 ml/min. Endothermic dehydration of gypsum occurs as follows: first, the adsorbed water is driven off, ending at around 105 °C, and then crystalline water is driven off in two stages—the first one ending at around 175 °C (forming CaSO4·½H2O), the second one ending at around 220 °C (forming unstable anhydrite III). The dehydration is complete and stable at about 250°C[30]. Endothermic decomposition of calcite occurs between 600 °C and 900 °C; the exact temperature depends on

Table 1 | List of samples of the interior stucco decoration and the analytical methods applied

ID	Sample	Element	Type of decoration/position	Figure	Analysis
STK 1	Finishing layer	clump of hair	relief sculpture—a nymph / Middle Hall	3 A	OM, SEM-EDS
STK 2	Finishing layer	leaf	high-relief decoration of the niche by phytomorphic shapes / Middle Hall	3 A	OM, SEM-EDS
STK 3	Complete stratigraphy	forearm of a putto	relief sculpture—a putto / North Hall	4 A	OM, SEM-EDS, TA, XRD, AD
STK 4	Complete stratigraphy	ears of wheat	low-relief background / North Hall	4 A	OM, SEM-EDS
STK 5	Complete stratigraphy	tail of a naiad	relief sculpture—a nymph / Middle Hall	3 A	OM, SEM-EDS, TA, XRD, AD
STK 8	Finishing layer	leaf	high-relief decoration of the niche by phytomorphic shapes / Middle Hall	3 A, 3B	OM, SEM-EDS
STK 10	Finishing layer	leaf	high-relief decoration of the niche by phytomorphic shapes / North Hall	4 A	OM, SEM-EDS, TA, XRD
STK 11	Finishing layer	leaf	high-relief garland above the garden entrance / North Hall	4 A	OM, SEM-EDS
STK 12	Finishing layer	leaf	high-relief decoration of the niche by phytomorphic shapes / North Hall	4 A	OM, SEM-EDS, TA, XRD
STK 13	Finishing layer	wall decoration panel, leafwork	low-relief / North Hall	-	OM, SEM-EDS
STK 14	Core modelling mortar	putto's body	relief sculpture—a putto / South Hall	2 A, 2B	OM, SEM-EDS, TA, AD
STK 15	Finishing layer	putto's finishing layer	relief sculpture—a putto / South Hall	2 A, 2 C	OM, SEM-EDS, TA
STK 18	Finishing layer	leaf	high-relief decoration of the niche by phytomorphic shapes / North Hall	4 A	OM, TA, XRD
STK 19	Finishing layer	leaf	high-relief decoration of the niche by phytomorphic shapes / North Hall	4 A	OM, SEM-EDS,
STK 20	Complete stratigraphy	wall decoration panel	low-relief / North Hall	4B	OM, SEM-EDS, TA, XRD
STK 22	Finishing layer	wall decoration panel, flower	low-relief / South Hall	-	OM, SEM-EDS

OM optical microscopy, *SEM-EDS* scanning electron microscopy, *TA* thermal analysis, *XRD* powder X-ray diffraction, *AD* acid dissolution.

the crystallinity, and the amount and type of calcium carbonate phase[31]. Before the XRD analysis, an internal standard (ZnO, 10 wt.%) was homogenized with the sample. Data were collected using Bruker D8 ADVANCE PRO diffractometer (Cu Ka radiation, 40 kV and 40 mA) with a step size of 0.01 °C in 2Θ and a counting time of 0.4 s/step. Crystalline and amorphous fractions were determined with the combined Rietveld-RIR method.

The proportion of insoluble residue (aggregate) was determined by dissolving a sample in an 8% solution of hydrochloric acid. Samples containing gypsum had to be dissolved in boiling hydrochloric acid (1:3) for about 2 min[32]. After dissolution, the aggregate was rinsed with distilled water several times. Sieve analysis was carried out to determine the particle size distribution of the dried aggregate. Subsequently, the mineralogical composition of each size fraction was examined under a stereomicroscope. In order to estimate the mixing proportions, the insoluble portion was attributed to the aggregate, while the soluble portion was regarded as binder. To estimate the mixing proportions between lime and gypsum, the ratios determined by thermal analysis were used. The following bulk densities were used for conversion to volumetric units: lime putty, 1300 $kg.m^{-3}$; dry hydrated lime powder, 740 $kg.m^{-3}$; sand, 1600 $kg.m^{-3}$; powdered gypsum hemihydrate, 900 $kg.m^{-3}$. The dry matter content of lime putty was 45%.

The presence of potential organic additives was assessed by means of nano-LC-TimsTOF mass spectrometry. Protein digestion and purification: 100–250 µL of 50 mM NH4HCO3 containing approximately 10 µg/mL of trypsin was applied to samples STK 3 A–C and left to react at room temperature for two hours. The solution was then purified using a reverse phase ZipTip. After the equilibrating, binding and washing steps, the target compounds were desorbed from the stationary phase. The solutions were subsequently used for nano-LC-TimsTOF analyses. The LC–MS/MS system consisted of a nanoElute 2 liquid chromatograph (Bruker Daltonics) coupled to a TimsTOF HT mass spectrometer (Bruker Daltonics). The purified and dried samples were resuspended in 50 µl of 3% acetonitrile with 0.1% formic acid. The mobile phase A was water with 0.1% formic acid, and the mobile phase B was acetonitrile with 0.1% formic acid. A volume of 1 µl of the resuspended sample was first loaded through a PepMap Neo-Trap trapping column (300 µm × 5 mm, Thermo Scientific) at 80 bar pressure using 100% phase A for 2.5 min. The sample was then eluted onto a PepSep C18 analytical column (75 µm × 100 mm, Bruker Daltonics). Peptide separation was carried out using a one-hour linear gradient of mobile phase B (3–35%). The eluted peptides were ionized using the Captive Spray 2 electrospray ionization technique. Data were acquired in Data Dependent Analysis (DDA) mode using Parallel Accumulation Serial Fragmentation (PASEF). The mass range was set to 100–1700 m/z. Ion mobility scans were performed in the range of 0.6–1.6 $V{\cdot}s{\cdot}cm^{-2}$, with a scan duration of 100 ms. Ten ion mobility scans were performed between two MS spectra. From the acquired data, peaklists were first extracted using DataAnalysis 6.1 software (Bruker Daltonics) and subsequently imported into the Proteinscape 4.2 proteomics data management system (Bruker Daltonics). Protein identification was performed using the Mascot search algorithm (version 2.4.1, Matrix Science), with the reference proteome of the corresponding organism downloaded from public biological databases (UniProt/NCBI) used as the search database.

Results

Macroscopic examination carried out on site and in the laboratory made it possible to distinguish the main layers of which the stucco decorations were composed of. Most of the samples were taken from the finishing stucco layer, including the applied surface finish and the subsequent coatings. However, for some samples, it was necessary to verify their structure and subsequently characterize the individual layers separately in the laboratory. For this purpose, samples STK 3, 4, 5, and 20 were divided into individual layers, which were additionally marked with capital letters A, B, C. By studying the stratigraphy of the putto's broken forearm, it was possible to infer the construction sequence of this relief sculpture, Fig. 5. The detached stucco fragment was about 8 cm in diameter and had an iron skeleton

element (forged roughly to 4 × 6 mm) encased in a gypsum layer of variable thickness of 4 to 15 mm. A sample of this material was labelled STK 3 A. This layer was clearly distinguishable from the subsequent layer, as there was a 'cold joint' between them—in some areas the two layers were not fully bonded. This indicated that the next layer was applied after the first had set. The second layer was between 10 and 40 mm thick. It consisted of several sub-layers that were very well bonded and not easily distinguishable, thus it was considered one material for the analysis. The sample of this layer was denoted STK 3B. A third layer was the final stucco layer. It was approximately 4 to 6 mm thick and was distinguishable by a finer structure (aggregate). The sample of this layer was labelled STK 3 C.

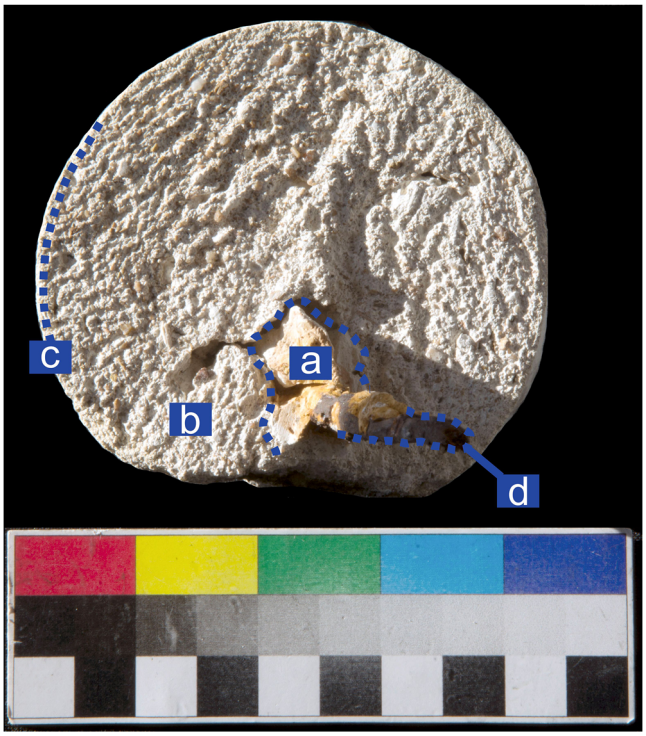

Fig. 5 | Section of the putto's forearm, raking light. a—gypsum layer, b—core mortar, c—finishing stucco, d—forged iron bar (4 × 6 mm).

The sculpture of a naiad was also made of at least two layers, the finishing stucco mortar (STK 1, hair; and the tail tip denoted as STK 5B), and core modelling mortar from the tail tip denoted as STK 5 A. Sample STK 4 from the low-relief background composed of wheat ears also included two layers, the core modelling mortar and the finishing stucco layer. Sample STK 20 from the low-relief wall panels comprised two different mortar layers, in this case a first coat (labelled STK 20B), a layer from which the plastic relief was modelled (STK 20 A), and an adjacent layer of a flat stucco without decorative elements (STK 20 C).

Optical microscopy (OM)

The whole set of samples is divided and described according to the functional layers of the stuccos. Subgroups with similar properties are further commented on based on the nature of their binding system, aggregate and structure.

Core mortar (samples STK 3 A, 3B, 4, 5, and 14) is a layer composed of a lime-gypsum binder with a predominance of the lime component, Fig. 6A. The binder in this layer is compact; pores and cracks are rare. Larger pores are mainly visible at the contact with the outer finishing stucco layer. However, the two layers are well connected. Binder related particles (BRP) occur in the matrix. These are usually uncracked compact lumps of fine-grained lime binder, 0.4–1 mm (maximum 2 mm) in size. Similarly, compact particles of gypsum or unburnt gypsum particles are dispersed throughout the layer. The lime-gypsum binder is well distributed; only rarely are there clusters of gypsum and lime that are not well dispersed, Fig. 6B.

The aggregate in the core mortar consists mainly of quartz clasts, both monocrystals and, less frequently, undulose grains. Feldspars and dark micas (biotite) are present as well. Fragments of fine-grained marble are also present in samples STK 3 A and STK 14. The grains in this layer are sharp-angled, irregular, and fractured; their size varies from 0.4 to 1 mm, with the largest up to 4 mm. The binder to aggregate (B/A) ratio, based on estimated volume percentage, is 1:1.

Sample STK 14 is different from the other core-mortar samples due to its inhomogeneous filler composition. In addition to single crystalline quartz

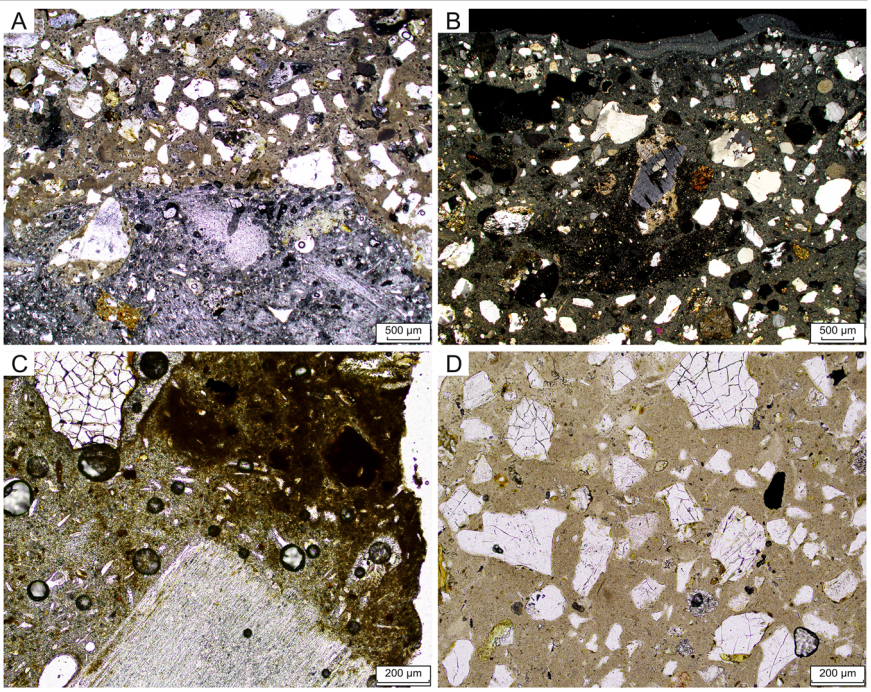

Fig. 6 | Transition between a lime-gypsum core mortar with a quantity of silica aggregate (upper layer) and a greyish coloured gypsum layer containing gypsum particles of varying degrees of processing (lower layer). Sample STK 3 A/B, PPL (**A**). A cluster of lime and gypsum in the core mortar. Single crystalline quartz grains are clearly visible in the surrounding matrix. Sample STK 5 A, XPL (**B**). An unprocessed gypsum particle (bottom) and cracked quartz grains of the aggregate (top). In the upper right corner, brownish to rusty discolouration of the matrix due to contact with the iron reinforcement. Sample STK 3 B, PPL (**C**). Fine-grained calcitic matrix with a siliciclastic filler composed of predominantly quartz grains, feldspars and dark micas (biotite). Sample STK 1, PPL (**D**).

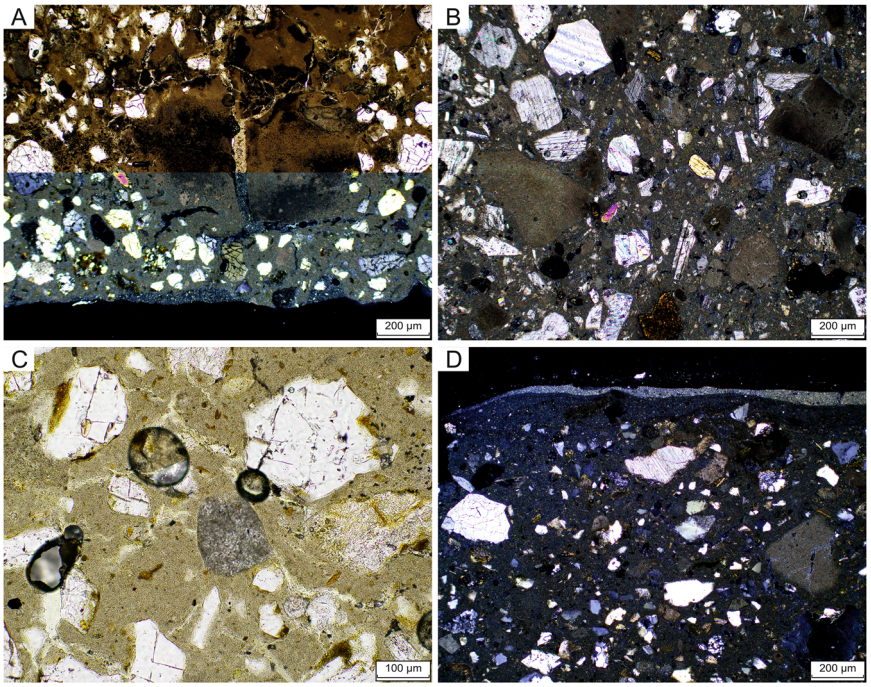

Fig. 7 | A BRP with the partially preserved fine-grained structure of the original raw material—limestone. Sample STK 2, PPL (upper half), XPL (lower half) (**A**). Distinctive sharp-angled fragments of coarse crystalline marble in a fine-grained calcitic matrix with BRPs. Sample STK 12, XPL (**B**). A finely crystalline limestone particle (center) with quartz grains in matrix, a possible relict of thermal disturbance. Sample STK 2, PPL (**C**). Stucco mortar with siliciclastic aggregates and crushed marble as a minor component. Sample STK 8, XPL (**D**).

grains, large grains and polycrystalline clusters are also abundant. The shape of the aggregate clasts varies for different fractions. The large grains are mostly oval, whereas the grains of the smaller size fractions are predominantly sharp-edged, irregularly shaped and cracked. The most frequent grain size of the fine-grained fraction is 0.3–0.5 mm, while the coarse-grained fraction has a typical size of 1–2 mm. Pores and cracks are more common in this sample than in the others.

The sample of the core mortar encasing the reinforcement (STK 3 A) is technically a part of this group but its composition and, as discussed later, its function are significantly different. This material is very rich in gypsum, which forms the matrix, Fig. 6C. It contains elongated gypsum particles of various sizes, most often 0.05–0.3 mm in size. The matrix is compact and free of pores and cracks. There is a stain with brownish to rusty hues at the point of contact with the iron reinforcement. The matrix contains whole and unbroken crystals of unburnt gypsum up to 3 mm in size. They have not undergone thermal alteration and have retained their original rock structure, Fig. 6C. Other clastic grains, namely quartz, feldspar or small micas (biotite), occur in quantities corresponding to 5–10%. These grains are sharp-angled, irregular and often highly fractured. The occurrence of coarse-grained gypsum particles is more frequent in this layer compared to the rest of the core modelling mortars.

Finishing stucco layer forms the outer mortar layer in the majority of the studied samples (STK 1, 2, 3 C, 4, 5, 8, 10, 11, 12, 13, 15, 18, 19, 20). It is composed mainly of fine-grained lime binder and fine aggregates, Fig. 6D. This layer is rich in BRPs with the most common particle size ranging from 0.5 to 1 mm, with the largest particles measuring up to 2.5 mm. The BRPs are fine-grained, usually compact, and in rare cases exhibit the partially preserved fine-grained structure of the original material, Fig. 7A. Samples STK 8 and 11 also contain a few particles of unprocessed gypsum; the presence of gypsum binder was, however, not identified. The layer is compact with no significant pores or cracks. As with the core mortar, the B/A ratio in this layer is typically 1:1 based on the estimated volume percentage. The samples from the stucco layer do not differ in the type of binder, but can be subdivided into subgroups based on their different aggregates.

There is a subgroup of stuccoes composed of lime and siliciclastic aggregate. For the stucco samples STK 1, 2, 3 C, 4, and 5, a typical siliciclastic aggregate composed of predominant quartz grains, feldspars (albite), dark micas (biotite) and accessory opaque minerals was identified, Fig. 7A. The shape of the grains is irregular, sharp-angled, and often cracked. The size of the grains varies from 0.2 to 0.8 mm, with the largest grains reaching up to 1.5 mm. All the samples in this subgroup show signs of higher grain sorting (compared to the other finishing stucco layers). In addition to the typical BRPs, finely crystalline limestone particles—up to 0.5 mm in size and irregular in shape with relics of thermal disturbance—occur in the binder as well, Fig. 7C.

There is a subgroup of stuccoes composed lime and siliciclastic aggregate, with crushed marble as a minor component. In addition to the main siliciclastic component of the aggregate, significant amounts of marble clasts are present in samples STK 8, 10, 11, 15 and 20, Fig. 7D. These are sharp-angled, irregular fragments of coarsely crystalline marble with frequent twinning of grains. The size of these fragments ranges from 0.2 to 0.4 mm, with the largest grains reaching up to 0.8 mm. The marble fragments differ in grain size from the siliciclastic ones present, which may indicate separate production and sieving of these two aggregates. Sample STK 10 exhibits lower grain sorting than the other stuccoes in this subgroup.

There is a subgroup of stuccoes composed lime and crushed marble, siliceous sand as minor component. The samples of the leaves decorating the niches in the North Hall (STK 12, 18, and 19) form a distinct subgroup due to the presence of crushed marble that replaces the siliciclastic aggregate, Fig. 7B.

The samples of the wall decoration panels (STK 13, 20) do not form a separate subgroup. Sample STK 20 is distinguished by a higher proportion of siliciclastic grains, mainly polycrystalline quartz fragments. Other properties of these samples do not differ from those of the finishing stucco layer.

Most of the samples included some kind of surface finish but two, STK 10 and 18, showed no coating layers; they retained only the finishing stucco layer surface finish. In contrast, the remaining samples revealed up to eight distinguishable layers comprising a combination of limewashes and paint layers.

Analysis of the surface stratigraphy showed a thin lime-dense layer, which is particularly noticeable in UV light, Fig. 8A–D, and in the BSE images, Fig. 9D. This is most likely the effect of smoothing the stucco with a metal tool, where the binder is pulled out to the surface with water. This layer is intact and had set and dried before the subsequent coatings were applied.

In all samples, the first coat of paint on the stucco was a limewash which typically consisted of two to three application layers. The transitions

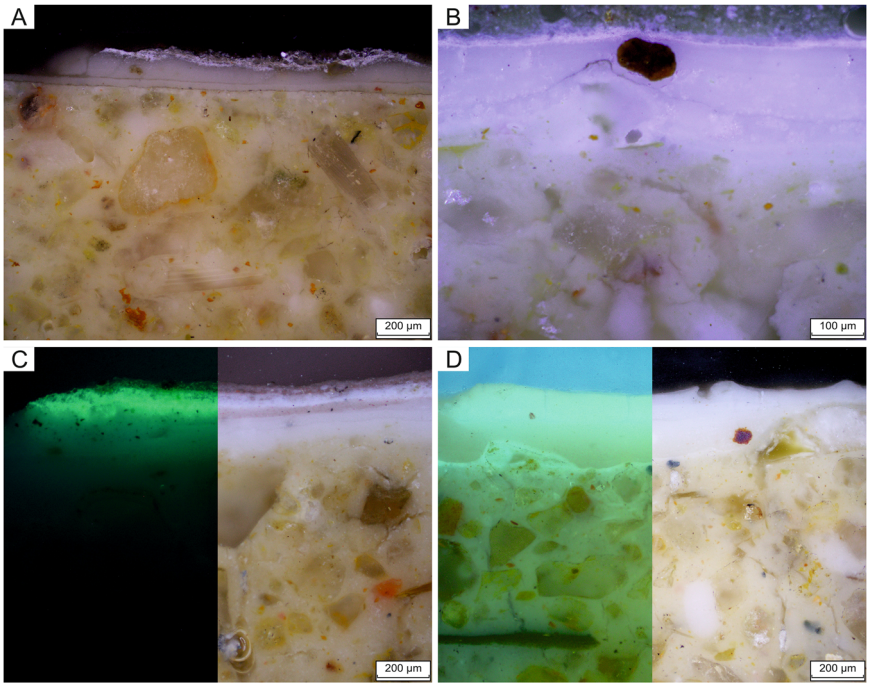

Fig. 8 | Thin black line on top of the finishing stucco layer covered with limewash. Sample STK 20 A (**A**). Reflected light. Black line on top of the first limewash layer. Sample STK 20 C. Reflected light (**B**). Strong luminescence of the white paint layer containing zinc white (ZnO). Sample STK 2. UV (left) and reflected (right) lights (**C**). Different luminescence of the first limewash compared to subsequent ones. Sample STK 3. UV (left) and reflected (right) lights (**D**).

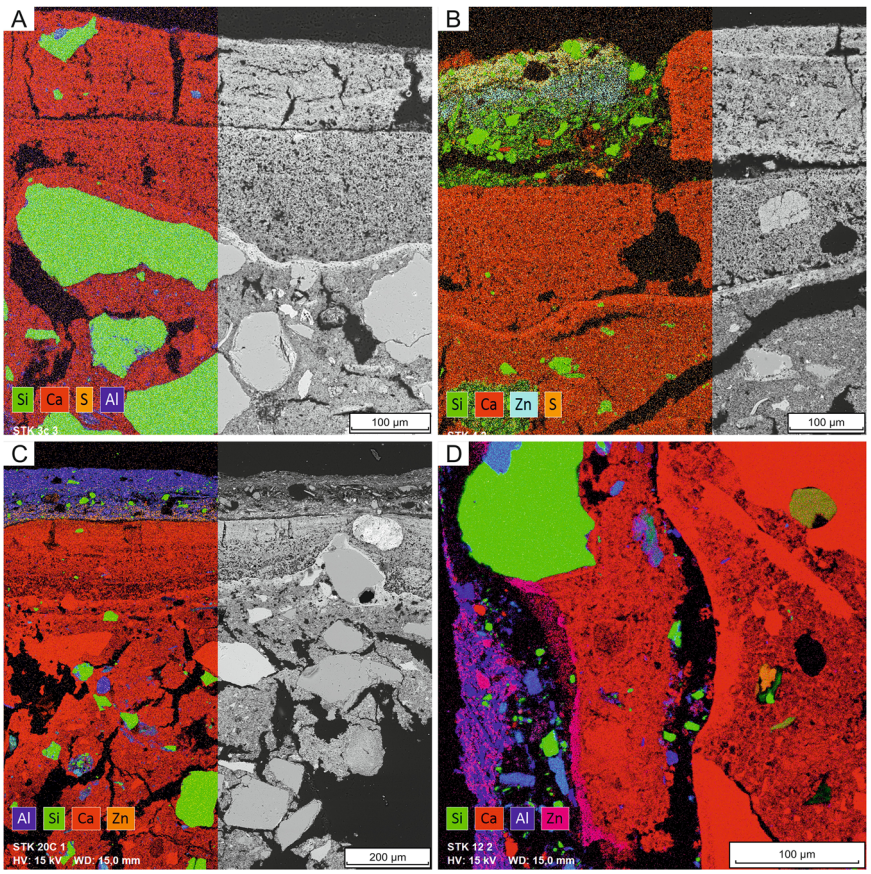

Fig. 9 | A thin layer with denser binder on top of the stucco is visible in the BSE image. The EDS map shows several limewashes. The first three application layers form the first limewash coating. Successive lime coatings are detached and cracked. Sample STK 3 (**A**). A thin layer with denser binder on top of the stucco visible in BSE image. Successive limewashes are detached from the first coating. The EDS map shows the presence of a zinc-oxide paint layer on top of a layer of deposits containing mainly silicates. Sample STK 4 (**B**). Two thin layers with denser binder present in the stucco. Differences in morphology between the first and the successive coatings. The EDS map shows the presence of zinc oxide and aluminosilicates in the upper layers. Sample STK 20 C (**C**). EDS map showing Si-rich deposits in the gap between mortar and limewash. Sample STK 12 (**D**).

between these application layers were barely perceptible, Figs. 8A–D, 9A–D, with both the optical and electron microscopes, indicating that the craftsman applied multiple layers of limewash wet-on-wet. In samples STK 3 and 4 a clear difference in luminescence in UV light was noted between the first limewash and the subsequent coatings composed of limewashes and paint layers, Fig. 8C, D. There are distinct morphological differences between the first and successive limewashes, the latter exhibiting more pronounced vertical cracks and weaker adhesion.

Table 2 | Average composition of the binding matrix of the main mortar layers and of the first coating layers

		CaO	MgO	SiO_2	Al_2O_3	FeO	SO_3	Minor elements	*N*
STK1 finishing layer	Matrix	95.1	0.5	1.8	0.4	0.2	1.4	Sr	6
	BRP (1)	98.7	0.2	-	-	-	1.1	-	6
	1st coat	97.8	0.4	0.8	-	-	0.7	Cl	3
STK 2 finishing layer	Matrix	97.3	0.7	1.3	0.2	-	0.3	Cl	4
	BRP (1)	99.2	0.8	-	-	-	-	Cl	4
STK 3 B—core mortar	Matrix	80.6	0.9	5.0	1.0	3.5	7.6	Na, Cr, Cl	10
STK 3 C finishing layer	Matrix	88.5	1.0	4.5	1.9	0.9	2.3	Cl	10
	1st coat	95.4	0.6	1.6	-	-	1.5	-	1
STK 4 finishing layer	Matrix	85.0	1.0	8.7	1.9	0.6	1.7	Na, Cl	5
	1st coat	95.3	0.8	1.2	-	-	1.6	Na, Cl	5
STK 8 finishing layer	Matrix	95.9	0.9	3.0	0.2	-	-	-	3
	BRP (1)	94.8	0.8	2.7	-	-	1.5	Na	6
	1st coat	93.5	0.4	4.6	-	-	0.8	Na	3
STK 11 finishing layer	Matrix	92.9	0.8	6.5	1.0	2.4	1.3	Na, Zr	19
	BRP (4)	95.9	0.5	2.6			0.5	Na	8
	1st coat[a]	21.1	1.4	53.8	12.2	3.6	3.7	Na, K	1
STK 12 finishing layer	Matrix	96.1	1.0	1.6	0.1		0.4	Na, Cl	9
	BRP (4)	96.4	0.8	1.5	-	-	1.0	-	4
	Marble (6)	99.8	0.2	-	-	-	-	-	6
	1st coat	97.2	0.8	1.3	-	-	-	Na, Cl	2
STK 13—finishing layer	Matrix	93.9	0.8	2.2	0.1	-	1.4	P	3
STK 15 finishing layer	Matrix	93.6	0.3	2.4	0.5	0.5	1.3	-	8
	BRP (1)	98.4	0.6	1.0	-	-	-	-	2
	1st coat	96.9	0.2	1.7	-	-	-	Na	3
STK 19 finishing layer	Matrix	96.8	0.5	1.0	0.2		1.2	Na, Cl	4
	BRP (4)	97.4	-	0.9	-	-	1.7	-	3
	Marble (3)	99.0	0.3	0.3	-	-	-	-	7
	1st coat	97.2	0.8	1.3	-	-	-	Na, Cl	2
STK 20 A finishing layer	Matrix	95.6	0.2	3.3	0.2	-	0.5	Na, Cl	6
	BRP (2)	98.3	0.3	0.7	-	-	0.75	-	2
	1st coat	51.5	1.1	27.4	9.9	4.6		Na, K, P, Ti, Cl	1
	2nd coat	97.7	-	1.9	-	-	0.4	-	3
STK 20 C—coarse intonaco	Matrix	97.2	0.2	1.9	0.3	-	0.3	Cl	6
STK 20 C—fine intonaco	Matrix	98.4	-	1.2	-	-	0.2	Na	4
	1st coat	98.5	0.3	1.3	-	-	-	-	2
STK 22 A—finishing layer	Matrix	98.8	0.5	0.6	-	-	0.4	-	3
	1st coat	97.0	0.6	1.2	0.4	-	0.8	Cl	3

Weight proportions in oxides (wt. %). The number in brackets refers to separate particles. *N* represents the number of analysed areas/points.
[a]The first layer (50–200 µm thick) on the stucco is not a lime wash.

In samples STK 12 and 19, representing the stucco made with crushed marble and a highly calcitic, exceptionally white binder, the first limewash coat is cracked and detached from the stucco finishing layer—resembling the secondary limewashes in samples STK 1–4. Additionally, localized dust deposits are visible between the stucco and the limewash, Fig. 9D.

Coloured coatings come as the third to fifth subsequent layers. Pigments are distinctly present in the pink (STK 2), grey (STK 4), beige (STK 20 C), and green (STK 22) paint layers; their compact structure confirms them as being intentional paint layers. In contrast, the loose structure of the ochre layer found in samples STK 4, STK 11, and STK 12, combined with the absence of a matrix to embed the pigments and create a paint layer, suggests that it is more likely a deposit than an intentional paint application. A thin black layer of deposits was observed in samples STK 20 A and C from the low-relief decorations. In the case of sample STK 20 A the black layer lies on top of the finishing stucco layer, while in sample STK 20 C, it lies on the first limewash, Fig. 8A, B. UV light examination of the cross-sections revealed the presence of a highly luminescent pigment, zinc white (ZnO), in the upper white and coloured paint layers, Fig. 8C, D.

SEM-EDS

The compositions of the binding matrices of the mortar samples, determined by means of EDS analysis, are compared in Table 2. All of the mortars contain a high proportion of CaO, which indicates the use of lime as the main binding agent. The SO_3 content in consistent with the addition of gypsum, and its elevated content was present in STK 3B, a core-mortar sample. A certain SO_3 content was detected in almost all of the mortars and

Table 3 | Mineralogical composition of the samples determined by XRD

Sample		Calcite	Dolomite	Gypsum	Quartz	Albite	Orthoclase	Microcline	Muscovite	Anorthite	Rutile
STK 3 A	Core mortar - reinforcement	9.8	-	87.7	2.4	-	-	-	0.1	-	-
STK 3 B	Core mortar	51.8	-	44.2	4.0	-	-	-	-	-	-
STK 3 B1	Gypsum particle	-	-	100	-	-	-	-	-	-	-
STK 3 B2	Undissolved particles	-	-	98.0	2.0	-	-	-	-	-	-
STK 3 C	Finishing layer	80.9	-	8.0	8.9	2.2	-	-	-	-	-
STK 5 A	Core mortar	59.7	0.7	32.3	4.4	1.7	-	1.9	-	-	-
STK 5 B	Finishing layer	83.8	0.4	1.1	8.3	-	-	4.1	2.3	-	-
STK 10	Finishing layer	70.7	-	1.5	17.9	3.4	2.0	-	2.2	2.3	0.1
STK 12	Finishing layer	96.9	-	-	1.4	-	-	-	1.6	-	0.1
STK 20 B	First coat	45.9	-	-	39.2	5.8	2.0		1.8	5.2	0.1

lime coatings, but this is more on the level of a contamination, as discussed later. The amount of MgO, as well as the levels of other impurities (SiO_2, Al_2O_3 and Fe_2O_3) that affect the properties of lime, is generally low in all the samples. Based on its composition, the lime binder in the samples can be classified as a calcitic air lime. A possible exception is sample STK 4, which, according to the determined elevated SiO_2 content may possess some hydraulic properties. Its binding matrix can be classified as feebly hydraulic. Within the air lime category, the matrix composition of some samples, namely STK 3B, 3 C, and 11, is more heterogeneous in silica content than others, potentially providing them with some hydraulic phases too. Apart from these exceptions discussed above, overall, the lime matrix composition is relatively consistent for all the mortars, BRPs and lime coatings. Other common features are high CaO, low MgO and silica-based impurities. The composition of the BRPs is generally purer than the surrounding binding matrix, suggesting that the elevated silica content present in some samples may originate from sources other than the lime binder used for mortar preparation. The crushed marble particles in samples STK 12 and 19 of finishing stucco layers contained exceptionally low amounts of impurities.

The chemical composition of the first limewash coat closely matches that measured for the BRPs, with a high CaO content of 96.7%, a low MgO content of 0.5% and variable quantities of SiO_2 and SO_3. The presence of Al_2O_3 was detected in minor amounts (0.4%) only in sample 22 A. The chemical composition of limewashes on the stuccoes with crushed marble (STK 12 and 19) is consistent, comprising 97.2% CaO, 0.8% MgO, and 1.3% of SiO2, with minor Na and Cl content.

Analysis of the samples using BSE images provides a more detailed view of the layers' morphology, including their compactness and adherence. In all the samples, a thin binder-dense layer is visible in the BSE images. Moreover, the surface of sample STK 20 C exhibits two of these layers, indicating that the stucco plaster has been reworked, Fig. 9C. EDS maps of samples STK 11, 12 and 19 reveal minor deposits between the layers, primarily composed of Si and Al, Fig. 9D. Additionally, all zinc-containing overpaints are clearly distinguishable. The zinc-white layer in sample STK 4 lies on top of an ochre deposit layer, Fig. 9. The two pink layers, identified in sample STK 2, showed a different chemical composition. The first layer is composed of calcium carbonate mixed with iron red, while the second layer consists of zinc white combined with iron red. The grey layer (STK 4) is rich in aluminosilicates. In sample STK 20 A, the beige layer is composed of zinc oxide and chromium yellow. For the green paint layer in STK 22, zinc white and iron pigments were utilized (organic additives cannot be excluded).

XRD-QPA

The mineralogical composition of the binder (fraction < 63 μm) determined by XRD is in line with the SEM-EDS analytical outputs, Table 3. Unlike the core mortar binder, which generally contains gypsum as a secondary binder (~30–45 wt.%), the STK 3 A sample of the mortar encasing the reinforcement is composed of gypsum with approximately 10 wt. % lime. The finishing stucco layer of the relief sculpture (STK 3 C) had about 10 wt. % of gypsum added to lime, which notably differs from the low relief (STK 5B) or leaves decorating the niches (STK 10 and 12), where the amount of gypsum is negligible or absent. Quartz, feldspars, micas, and rutile originate from the fine fraction of aggregate. Their variable amounts are caused by the preparation of the sample, which must be finely crushed to separate the binder. The nearly 40 wt. % of quartz in sample STK 20B, however, is unusually high across all samples studied. The XRD of the rounded particles (STK 3B1), which were manually separated from the gypsum and lime-gypsum-based matrices, confirmed that they were composed of gypsum. The white particles (STK 3B2), which were not dissolved by the acid attack (8% HCl), were also gypsum-based as confirmed by the XRD analysis.

Thermal analysis (TA)

Two main processes were identified by TA corresponding to the dehydration of calcium sulphate dihydrate (between 50 °C and 200 °C) and the decomposition of calcium carbonate (between 600 °C and 850 °C). Their weight loss values were used to quantify the proportions of gypsum ($CaSO_4.2H_20$) and lime ($CaCO_3$), as shown in Table 4. The analysed samples (sieved below 63 μm) were not solely composed of a binder but also included a variable amount of the finest-fraction aggregate compounds as confirmed by XRD. The presence of the fine aggregate influenced the quantified values of the binders, especially in the case of samples STK 14, 10, 15, and 20B where the aggregate contamination was higher. Weight losses within the temperature range of 200–600 °C are comparatively low, 1.2–3 wt.%, indicating a small amount of structurally bound water, Fig. 10. These observations confirm the use of non-hydraulic lime and imply that the water released within this temperature interval most likely originates from clay inclusions, hydrated iron compounds or inorganic salts. Samples of the core mortar are all composed of a mixture of gypsum and lime in various proportions. The slight shifts in dehydration and decomposition peaks could be due to the presence of variable amounts of unprocessed gypsum and lime particles. This effect is clearly observable in the analysis of sample STK 12, which contains crushed marble aggregate, where the carbonate decomposition peak shifts to a higher temperature. However, it is not possible to quantify the amounts related to unprocessed particles; only a qualitative estimate based on optical microscopy can be made.

Dissolution and sieve analysis

The insoluble residue and the ratio of calcium carbonate to calcium sulphate obtained from the thermal analysis were used to calculate the mixing proportions of the mortar. Based on the weight proportions, the volumetric proportions were estimated using approximate bulk densities of the materials, Table 5. As it is generally assumed that the raw materials were dosed in batches using building ladles or similar tools available on site, the mixing ratio was expressed in volumetric units. The simplified average proportions of the core modelling mortar could be approximately 1 to 1 for lime putty and sand with gypsum varying from 0.3 to 0.5. In the case of the final stucco mortar mixture, only one sample was suitable for the test and the ratio was 1

Table 4 | Results of thermal analysis—weight loss due to gypsum dehydration and carbon decomposition

	weight loss (%wt.)			(% wt.) by TG		(% wt.) by XRD-QPA		
	50–200 °C	200–600 °C	600–850 °C	$CaSO_4.2H_2O$	$CaCO_3$	$CaSO_4.2H_2O$	$CaCO_3$	
STK 3 A	17.35	1.22	3.64	81.8	8.30	87.7	9.8	Core mortar
STK 3B	7.61	2.95	23.33	33.3	53.0	44.2	51.8	
STK 5 A	6.23	2.64	23.31	27.2	53.0	32.3	59.7	
STK 14	3.03	2.18	17.16	14.5	39.0	-	-	
STK 3 C	2.39	3.36	29.65	7.9	67.4	8.0	80.9	Finishing stucco mortar
STK 5B	1.08	3.73	32.55	2.3	74.0	1.1	83.8	
STK 10	0.65	3.00	28.23	0.0	64.2	1.5	70.7	
STK 12	0.31	1.98	39.79	0.0	90.4	-	96.9	
STK 15	0.75	2.56	22.16	1.5	50.4	-	-	
STK 20B	0.49	2.48	20.29	0.0	46.1	-	45.9	

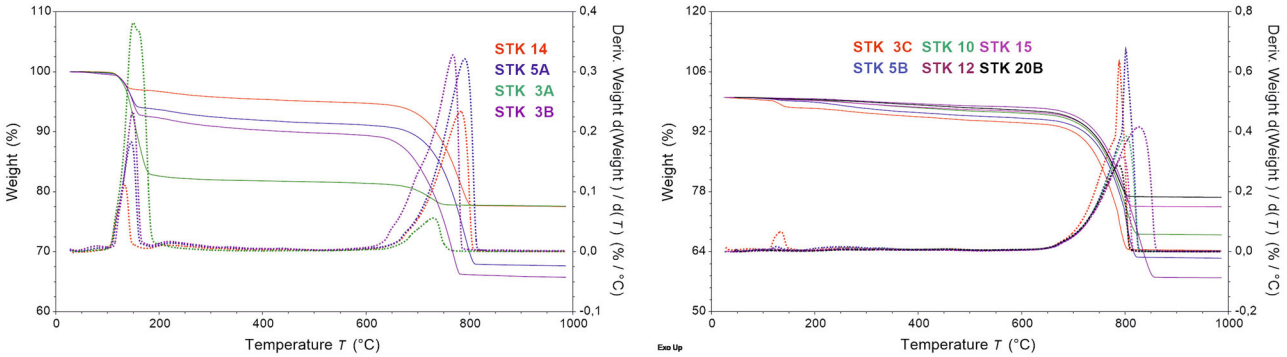

Fig. 10 | Results of thermal analysis. TGA and DTG curves of the core modelling mortar (left) and the finishing stucco mortars (right).

Table 5 | Estimated mixing proportions of the core modelling mortar and the final stucco mortar in volumetric proportions

	STK 3B		STK 5 A		STK 14		STK 5B	
Undissolved residue (wt. %)	58.0		59.1		50.4		55.3	
$CaCO_3/CaSO_4.2H_2O$ ratio (-)	1.6		2		2.7		-	
	putty	powder	putty	powder	putty	powder	putty	powder
Lime	1		1		1		1	
sand	1.1	1.4	1.1	1.4	0.7	0.9	0.6	0.8
Gypsum	0.5	0.6	0.4	0.5	0.3	0.3	-	-

to 0.6 of lime putty to sand. The samples with gypsum that at first did not dissolve completely had to be treated with boiling acid. The undissolved gypsum particles are visible in Fig. 11. The gypsum-bearing layers are characterised by whitish and rounded gypsum clusters that form rounded insoluble particles. In general, the 0.25–0.5 mm fraction dominates in size, with the 0.5–1 mm and 0.125–0.25 mm fractions being less represented.

The mineralogical analysis shows that a very similar sand was used for both the core modelling mortar and the finishing stucco mortar. The predominant components are quartz grains of various colours. Less common are rock fragments (gneiss) composed of quartz, as well as feldspars (albite) and micas (biotite). The individual sand clasts are angular (sometimes slightly rounded) but rather unworked with an uneven surface. The shape, roundness and overall sorting of this material suggest that transport of this sand probably took place only a short distance from the source rock. The main difference in the selection of sand for the core mortar and the finishing stucco mortar is the content of fine particles. Microscopic analysis of most of the samples shows that the main size range of the finishing stucco mortar sand is around 0.2–0.8 mm and a maximum grain is usually no larger than 1 mm, exceptionally reaching up to 2 mm. The sieve analysis also shows that the amount of the fine fraction (<0.063 mm) differentiates this sand from the one used in the core mortar.

Protein analysis by nano-LC-TimsTOF mass spectrometry

The proteomic analysis of sample STK 3 from the putto's forearm was conducted on this representative sample because it comprises three distinct mortar layers and originates from the most artistically advanced form. The results show that samples STK 3 A and C do not contain any proteinaceous additive. Sample STK 3B contains some matching peptide chains of ovalbumin and collagen, Table 6. Due to the low number of peptides, the result is inconclusive as the identified proteins from egg and animal glue could also originate from contamination. Further analysis would be required to confirm the presence of such additives. No relevant plant proteins were found.

Discussion

The discussion addresses the primary focus of the research–the understanding of the materials and techniques of stucco production.

Regarding the materials of the stucco mortars, the lime binder used was of fairly uniform quality and exceptionally pure with very low amounts of

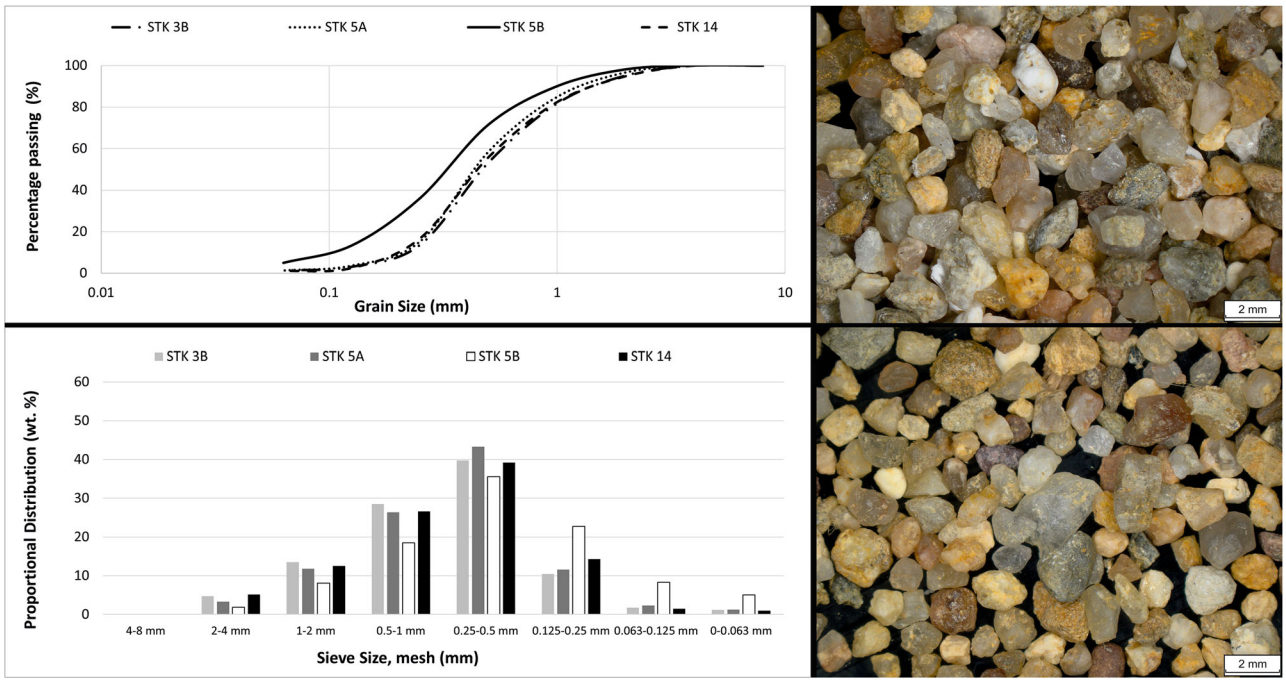

Fig. 11 | Particle size distribution of the aggregate and the 1–2 mm fractions of sand after the dissolution of the mortars with 8% HCl, samples STK 5 A (upper) and STK 5 B (lower). The white particles in sample STK 5 A are gypsum.

Table 6 | Protein identification in sample STK 3 B

Accession	Protein	#Peptides
FETUA_BOVIN	Alpha-2-HS-glycoprotein	3
K2C1_HUMAN	Keratin, type II cytoskeletal 1	3
K22E_HUMAN	Keratin, type II cytoskeletal 2 epidermal	2
OVAL_CHICK	Ovalbumin	2
K1C10_HUMAN	Keratin, type I cytoskeletal 10	2
ALAT2_DANRE	Alanine aminotransferase 2-like	2
DCPS_PIG	m7GpppX diphosphatase	2
NPAP1_HUMAN	Nuclear pore-associated protein 1	2
CO4A6_HUMAN	Collagen alpha-6(IV) chain	2
DAAF1_DROPE	Dynein assembly factor 1, axonemal homolog	2

MgO, SiO_2, Al_2O_3 and Fe_2O_3. No hydraulic compounds were detected, and EDS analysis revealed that the $CaCO_3$ content consistently exceeded 90 wt. %. The only exception is sample STK 4, where the elemental composition of the binder corresponds to slightly hydraulic lime. However, this is based on only a small measurement area, and the use of such lime has not been confirmed in the other samples.

The structure, BRPs present, and general character of the STK4 binder is similar to the rest of the samples, and the different chemical composition is most likely due to natural heterogeneity in the raw material. The use of a highly calcitic limestone was also confirmed by the composition of the BRPs, which are even purer than the matrix itself. The remnants of the original material structure in the BRPs suggest that a fine-grained limestone was used for the burning including the STK 4 sample.

The main local sources of limestone are known from the estate accounting books. The chemical purity and fine-grained structure points to the locations near Přerov, where a high-quality Devonian limestone is available. Another potential source, also widely available to the estate, is Jurassic limestone from Kurovice, which, however, contains high levels of impurities, Fig. 12.

Archival sources suggest that the lime was most likely produced locally. Wood-fired lime kilns were typical of the time, and if properly managed, the lime was expected to be soft-burnt and free of ash and charcoal[33,34].

The compactness of the matrices and controlled size of the BRPs seem to exclude the use of any type of hot mixing. The binding matrix also contains small, fine crystalline limestone particles structurally corresponding to Devonian limestone from Přerov and can thus be regarded as under-burnt remnants. The presence of these particles, as well as the high density of the material, could suggest that a dry-slaked lime powder was mixed with sand and possibly also with gypsum powder before water was added[6,35]. However, other mortar preparation methods that would include sieving of the binder (limiting the maximum sizes) and leaving behind heavier unprocessed limestone fragments cannot be ruled out. Moreover, archival documents state that lime was burnt in August to be ready for use in spring 1688[14]. The practicality of storage would suggest that lime was stored in lime pits to mature.

Gypsum was imported in advance from Ketř[14], and the rocks were probably quite pure with few contaminants, as indicated by the analysis of STK 3 A. A rare archival reference connected to B. Fontana's work in Vyškov[36] suggests that the gypsum was burnt in a kiln built by local craftsmen. The wording implies that building such a kiln was a routine task requiring no special explanation. The type and design of such a kiln remain unknown due to the lack of archaeological evidence and detailed studies. The gypsum rocks from the Ketř-Opava basin (a Middle Miocene calcium-sulphate-dominated evaporite area in the northern Carpathian Foredeep[37] form friable crystal clusters. Kilns similar to flare lime kilns (but with open fronts) would likely be impractical due to the incoherence of the rock[38]. A more suitable method of dehydration would therefore be cooking or baking the crushed stone in pots or pans. The presence of anhydrite, a typical product of burning at higher temperatures than ~350 °C, was not identified by XRD or by microscopy. Additionally, there was an abundance of unprocessed gypsum particles and rock fragments in the mortars. This indicates that the gypsum was most likely burnt at relatively low temperatures, producing mostly hemihydrate with some portion of under-burnt material. It remains unclear when and how the gypsum was crushed and ground to powder. Generally, crushing burnt gypsum is less energy-intensive because it becomes softer[38].

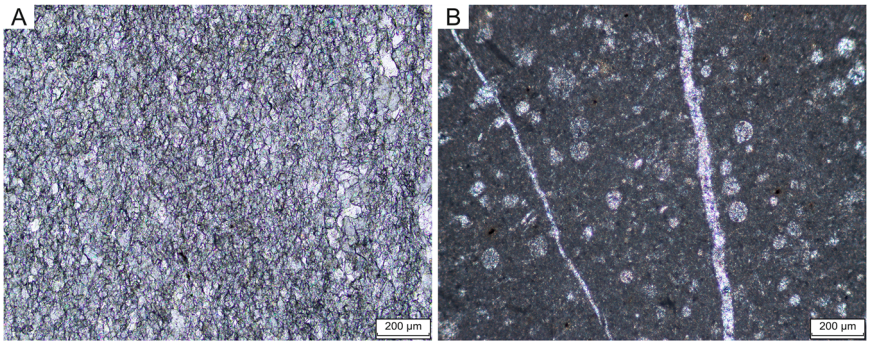

Fig. 12 | Structure of Devonian crystalline limestone from the Žernovy quarry near Přerov, XPL. **A** Jurassic Kurovice limestone with calcitic bioclasts and veins, XPL (**B**).

The main aggregate used was siliciclastic sand, most likely of local origin. It came from fluvial sources and had very similar characteristics although the fine and coarse sands were likely quarried from separate deposits. The fine sand is not merely a smaller size fraction of the coarse one. Both sands were most likely sieved to achieve the desired grain size. The analysis indicates that grain size was chosen according to the intended use. The finishing stucco layer had grains typically under 1.5 mm and contained a certain portion of a fine fraction (<0.063 mm); the core mortar had sand up to 4 mm and had a very low content of the fine fraction. There is also variability between samples, likely reflecting differences in natural resources or shifts in material supply/production timing. This is evident in sample STK 14 (core mortar from the putto in the South Hall), which features more heterogeneous sand compared to samples STK 3, 4, and 5 from the North Hall.

The marble in the stucco finishing layers was produced by crushing a metamorphic limestone that differs from the fine-grained Devonian limestone used to produce lime and even more from the Jurassic limestone of Kurovice. The exact origin of this limestone has not been identified. However, similar marble was quarried in Nedvědice in Southern Moravia–a location that was well known to the estate, as marble for architectural elements and sculptures was obtained there.

Considering the execution of the stucco decoration, the samples were divided according to the stucco parts from which they were taken, i.e., relief sculptures, low relief, high relief, and wall panel decoration, for the purpose of comparing mortar mixtures with different functions. Except for the relatively flat wall panels, all three-dimensional stucco decorations were made as layered structures, where the main shape was modelled from a lime-gypsum-sand mortar mixture. The level of detail in the modelling was high and included not only correct proportions but also finer surface work. It seems that the more artistically demanding works were modelled almost to perfection, as only a very fine layer (about 3–4 mm thick) of finishing stucco mortar was used on the forearm of the putto (STK 3), compared to the more repetitive fruit and floral motifs, where the thickness of the finishing stucco was more variable. This may indicate that different workers, with different modelling skills, were employed depending on the complexity of the decoration.

The core mortar is composed of lime, gypsum and sand. The calculated volumetric mixing proportions (lime putty, gypsum, sand) were 1:0.4–0.5:1.1 in the North Hall and 1:0.3:0.7 in the South Hall. The typical/maximum grain sizes of sand were 0.4–1 mm/4 mm, lime-based BRP were 0.4–1 mm/4 mm, and gypsum particles were 0.05–0.1 mm/3 mm.

The finishing stucco mortar is composed of lime and sand. Its volumetric mixing proportions were 1 : 0.6 (lime putty to sand). The typical/maximum grain sizes of sand were 0.2–0.8 mm/1.5 mm, lime-based BRPs were 0.5–1 mm/2.5 mm, and crushed marble particles were 0.2–0.4 mm/0.8 mm.

The skeleton of the relief sculpture, in the case of the studied putto, is made of forged iron. The first layer composed of gypsum mortar with a very low amount of lime, was applied directly onto the iron. This layer served as a bonding bridge between the iron and the core modelling mortar, which significantly stiffened the entire skeleton. While this hypothesis cannot be verified through material analysis, the mass of the successive layers suggests that a solid base was absolutely necessary. The main body mass was modelled in layers until he desired shape and proportions were reached. The layers were not regular but were very well bonded; their interfaces were visible only in some sections. This indicates wet-on-wet application until the body part was completed in a single stage.

The mortar contained lime and gypsum in proportions varying from 1.6 to 2.7. The gypsum was present as coarsely ground hemihydrate with numerous under-burnt particles. Since hemihydrate sets quite rapidly, some additives were likely used to slow down the setting time. It was common at the time to use animal glue for this purpose[39,40]. The analysis of organic additives suggested that animal glue may have been present in the core mortar; however, definitive proof based on a larger dataset was beyond the scope of this survey and remains a task for future research. A method involving repetitive reworking of the gypsum-lime mixture to prolong plasticity is also assumed but no structural evidence supports this in the current samples. One isolated cluster of gypsum mixed with lime, seen in sample STK 5, is likely only a result of improper mixing.

Differences in mortar composition for the same type of stucco may reflect either the work of different teams, variability in raw material supplies, or even different phases of execution. Of particular interest is the variable use of crushed marble. It is present in finishing stucco samples STK 8, 10, 11, 12, 15, 18, 19, and 20. Crushed marble completely replaced the siliciclastic aggregate in the North Halls niche garlands (samples STK 12, 18, and 19). A shortage of marble is unlikely, so its addition seems to document a deliberate change in recipe. Addition of crushed marble provides a whiter, more light-reflective surface, so its inclusion may have been influenced by aesthetic intentions. Information on the stucco making over the course of time is not available, but if we assume that the addition of marble represents an improvement, then stucco without it would be the earlier work. Interestingly, the North Hall garlands are slightly less rich in decoration, asymmetrical, and exhibit a noticeable change in pattern at a certain height–possibly due to a scaffolding or other obstacles. Another point to consider regarding this technological change is that these stuccoes were likely made by a different group of craftsmen, perhaps even without involving B. Fontana's workshop. In Fontana's later decoration of the Gallery of Angeles at Uherčice Château (1692–1969) crushed marble was not used, even though it was apparently available, as evidenced in the study by Uccelli et al.[5].

Travelling craftsmen and artists had to adapt to the local materials available. This is known from contracts and accounting records that document acquisition and purchase of materials[14]. Interestingly, these materials are described in general terms, without any specific quality demands. The estate most likely secured the best materials available within reach, so quality was not seen as an issue. Rare notes refer to technological processes; for example, a 1688 record states that "…lime was procured and slaked in August and put out for the next year"[14]. Whether the lime was stored in pits and used as a putty, as generally assumed, or in the form of powdered hydrate remains unknown as discussed earlier. However, this was

before B. Fontana and his team were commissioned to carry out the stucco decorations[18].

The material analysis shows a clear preference for pure lime with high calcite content. This was a deliberate choice, as it came from a source that was not the most readily available. It is known that the quality of lime depends not only on the raw material but also on the production processes such as burning, slaking, and storing, all of which significantly affect the final product[33,41]. While material analysis cannot unambiguously determine the production method, it can highlight characteristic properties associated with it. Some features potentially linked to particular skills of *stuccotori* include:

The compactness and the minimum shrinkage cracks of the finishing stucco layer indicate the use of procedures that allowed for precise control of water content in fresh mortars. For the determined mixing proportions of the finishing stucco mortar, the matured lime putty would, however, contain too much water to achieve suitable workability. There are therefore two possibilities: either the putty or the subsequent mortar was somehow dewatered, or dry-slaked lime powder was used and the right amount of water was added to adjust the required workability.

Gypsum binder, when used alone or with a minimal lime content, was coarsely ground and included unprocessed particles up to 3 mm in size. Despite this coarse texture, the resulting binding matrix was compact and effectively served the purpose of fixing the structural skeleton and bridging it with the next mortar layer. The coarse grinding was likely considered adequate—possibly even beneficial—for this application. When gypsum was combined with lime to prepare the core modelling mortar, a slightly finer gypsum fraction was employed.

Each mortar component was intentionally sized below a certain grain threshold, tailored to its specific role. For the finishing stucco mortar, most of the sand grains were smaller than 1.5 mm, while crushed marble particles were limited below 0.8 mm. This suggests that these aggregates were individually prepared and selectively added. BRPs in the fine stucco were the largest particles with a maximum size found about 2 mm, confirming that the lime was also processed in a different manner.

Coarser sand was chosen for the core mortar, where greater volume and structural mass were needed to model the shape. This practice aligns with traditional construction techniques—larger grain sizes help mitigate shrinkage and enhance mechanical strength.

Lime-to-gypsum ratios in the core modelling mortar ranged from ~1.6 to 2.7. It is likely that gypsum was added intuitively, based on practical, on-site requirements such as the desired setting time, the weight of element being modelled, and its spatial position. This flexible, experience-based approach was common among other master plasterers from Ticino, who were renowned for their expertise in the field. B. Fontana, who originated from the same region, likely shared and employed similar practices[42].

Based on the morphology and chemical composition of the coatings, it may be assumed that the initial decorations consisted of white limewashes only, applied in a variable number of layers with variable thicknesses. Coloured layers came as successive modifications. It is evident that all of the surface coatings were applied to dry mortar. The uniformity observed in the first two to three application layers of the first coat, characterized by similar luminescence under UV light, strong adhesion, and in some cases indistinct borders, suggests that the limewash was applied in multiple layers, typically up to three. The first layer was usually thicker, indicating that a thicker, less diluted limewash was likely used compared to the subsequent layers. The limewash rendered the stucco a completely purely white, although the underlaying surface texture, whether rough or smooth, most likely remained visible. Tonal variations between different parts of the decoration may have been achieved by adding further whitewashes of varying thicknesses.

As for the stucco samples STK 12 and 19, which contained crushed marble, considering the similarities in morphology and chemical composition of the first limewashes, it can be inferred that these coatings are different from the rest of the studied samples. Deposits beneath these coatings suggest that they were applied at a later time than the other lime coats (which can be regarded as original). This suggests that stucco containing crushed marble may have been intentionally left uncoated, possibly to make the most of the material's unique lustre. Based on only one sample (STK 20 A) from the low-relief leaf on the wall panel, it can be assumed that originally the specific colour of the stucco finishing layer could have also been used as the final decoration. This hypothesis would need to be confirmed by further studies. The coloured layers–pink (STK 2), grey (STK 4), beige (STK 20 C) and green (STK 22)–are secondary interventions, while the ochre layers (STK 4, 11, and 12) were interpreted as being deposits. In the secondary paint layers, zinc white is predominant. Its presence allows for approximate dating of these layers to post 1780, and most probably after the 1830s[43].

Future material analysis and archival findings can provide further insights into some of the open questions identified here and will continue to support the understanding of the materials and techniques of the high-Baroque stucco decorations. A more statistically significant number of samples would be required to confirm the use of organic additives into the gypsum mixtures and additional research can extend the acquired knowledge, e. g., provenance studies can be improved by analysis of the isotopic content of Sr, C and O, the presence of hydraulic compounds in STK 4 can be verified, or pH profiling of mortar layers can be used to corroborate non-hydraulic lime. Raw datasets, thin-sections and samples are stored at ITAM CAS and are available for follow up studies upon reasonable request.

Data availability

Raw datasets, thin-sections and samples are stored at ITAM CAS and are available for follow-up studies upon reasonable request.

Received: 25 June 2025; Accepted: 16 October 2025;
Published online: 28 November 2025

References

1. Rampazzi, L. et al. The stucco decorations from St. Lorenzo in Laino (Como, Italy): The materials and the techniques employed by the "Magistri Comanchini. *Anal. Chim. Acta* **630**, 91–100, https://doi.org/10.1016/j.aca.2008.09.052 (2008).
2. Rampazzi, L. et al. The stucco technique of the Magistri Comacini: The case study of Santa Maria dei Ghirli in Campione d'Italia (Como, Italy). *Archaeometry* **54**, 926–939, https://doi.org/10.1111/j.1475-4754.2011.00651.x (2012).
3. Caroselli, M., Zumbühl, S., Cavallo, G. & Radelet, T. Composition and techniques of the Ticinese stucco decorations from the 16th to the 17th century: results from the analysis of the materials. *Herit. Sci.* **8**, 1–20, https://doi.org/10.1186/s40494-020-00446-4 (2020).
4. Caroselli, M. et al. Study of materials and technique of late Baroque stucco decorations: Baldassarre Fontana from Ticino to Czechia. *Heritage* **4**, 1737–1753, https://doi.org/10.3390/heritage4030097 (2021).
5. Uccelli, M. et al. Characterization of the stucco decoration by Baldassarre Fontana in the Gallery of the Angels at Uherčice Château (CZ). *J Archaeol Sci Rep.* **44**. https://doi.org/10.1016/j.jasrep.2022.103493 (2022).
6. Válek, J. et al. Composition and technology of the 17th century stucco decorations at Červená Lhota Château in Southern Bohemia. *Int. J. Archit. Herit.* **14**, 1–16 (2020).
7. Beard, G. Stucco and decorative plasterwork in Europe. (Thames & Hudson Ltd, 1983).

8. Millar, W. Plastering plain and decorative. 4th ed. (Taylor & Francis Ltd., 1897). Reprint 2010.
9. Groot, C., Ashall, G. & Hughes, J. Characterisation of Old Mortars with Respect to their Repair, State-of-the-Art Report of RILEM TC 167-COM, (RILEM publications S.A.R.L., 2007)
10. Paladio, A. Quattro Libri dell'Architettura. Venice: Apresso Bartolomeo Carampello. (1581).
11. Scamozzi, V. L'Idea dell'Architettura Universale. Venezia: per Girolamo Albrizzi. Reprint of 1615 edition. (1714).
12. Vasari, G. Vasari on technique. London: J.M. Dent & Comp. Translated from the original published in 1550. (1907).
13. Alberti, L. B. Ten books on architecture. London: Alec Tiranti. Translated from the original published in 1755. (1965).
14. Peřinka. F. V. History of the City of Kroměříž II/1-2. History from 1619 to 1695. (In original: Dějiny města Kroměříže II/1–2. Dějiny let 1619–1695) Kroměříž. (1948).
15. Orálková, Z., Topičová, S. & Kouřil, K. The communication network of Bishop Karl of Liechtenstein-Catelcorn 1624–1695. (In original: Komunikační síť biskupa Karla z Lichtensteinu-Catelcorna 1624–1695.) (Olomouc, 2019).
16. Daniel, L., Perůtka, M. & Togner, M. Archbishop´s Chateau & Gardens in Krom. *ěříž, Kroměříž.*, (2019).
17. Kroupa, J., Pavlíček, M., Štětina, J. & Zapletalová, J. Reconstruction of the Residence in Kroměříž, 1664–1668, 1687–1698, in: R. Švácha, M. Potůčková, J. Kroupa (eds.), Karl von Lichtenstein-Castelcorno (1624–1695). Places of the Bishop´s Memory, Olomouc, pp. 97–154. (2019).
18. Zapletalová, J. The ground halls of the castle in Kroměříž and designs for sculptures for the castle gardens. (In original: Salyterreny zámku v Kroměříži a návrhy soch pro Podzámeckou zahradu. Jana Zapletalová. Umění / Art. 65, 269–282 (2017). .
19. Zapletalová, J. Fedele Raggi, Romanus sculptor in Moravia, Umění / Art, Praha: ČASV 73: 47–56. https://doi.org/10.54759/ART-2025-0103 (2025).
20. Arslan, E. (ed.). Arte e artisti dei laghi lombardi, II, Gli stuccatori dal barocco al rococo, Como. (1964).
21. Zapletalová J. Artists from the Lombardy-Ticino Lake Region in the Service of Bishop Karl von Lichtenstein-Castelcorno. O. Jakubec (ed.), *Karl von Lichtenstein-Castelcorno (1624–1695). Bishop of Olomouc and Central European Prince*, Olomouc, Olomouc Museum of Arts. pp. 179–190. (2019).
22. Zapletalová, J. Artists from Lake Lugano and nearby regions in the Czech lands as bearers of expertise in the creation of stucco decorations. (In original: Umělci od Luganského jezera a z blízkých regionů v českých zemích jako nositelé know-how realizace štukových dekorací. P. Waisser (ed.), Renaissance and Mannerist Stucco Work in Bohemia and Moravia, Olomouc, pp. 36–47. (2022).
23. Damiani Cabrini, L. Le migrazioni d'arte. R. Ceschi (ed.) Storia della Svizzera italiana. Dal Cinquecento al Settecento: Bellinzona. pp. 289–312. (2000).
24. Máčelová, L. Baldassare Fontana in Moravia. (In original: Baldassare Fontana na Moravě.) (dissertation thesis), Masaryk University in Brno, Faculty of Arts, Brno. (1949).
25. Karpowicz, M. *Baldasar Fontana 1661–1733. Un berniniano ticinese in Moravia e Polonia* (Lugano, 1990).
26. Karpowicz, M. *Baltazar Fontana*, (Warszava, 1994).
27. Kurzej, M. Depingere fas est. Sebastian Piskorski as both designer and provisional administrator. (In original: Depingere fas est. Sebastian Piskorski jako konceptor i prowizor), (Kraków, 2018).
28. Elsen, J. Microscopy of historic mortars—a review. *Cem. Concrerte Res.* **36**, 1416–1424 (2006).
29. Boynton, R. S. Chemistry and technology of lime and limestone. 2nd edn. (Wiley, 1979).
30. Engbrecht, D. C. & Hirschfeld, D. A. Thermal analysis of calcium sulfate dihydrate sources used to manufacture gypsum wallboard. *Thermochim. Acta* **639**, 173–185, https://doi.org/10.1016/j.tca.2016.07.021 (2016).
31. Földvári, M. Handbook of thermogravimetric system of minerals and its use in geological practice. Budapest: Geological Institute of Hungary. Occasional Papers of the Geological Institute of Hungary. (2011).
32. Middendorf, B., Hughes, J. J., Callebaut, K., Baronio, G. & Papayianni, I. Investigative methods for the characterisation of historic mortars—part 2: chemical characterisation. *Mater. Struct.* **38**, 771–780, https://doi.org/10.1007/BF02479290 (2005).
33. Válek J. et al. Lime technologies of historic buildings. (In original: *Vápenné technologie historických staveb.)* (Praha: NTM, V). pp. 168.
34. Wingate M., Sakula J. & Hill N. *Small-scale Lime Burning: A Practical Introduction*. (Intermediate Technology Publications, 1985).
35. Válek J. et al. According to the old model: reconstruction of mortar, sgraffito, and stucco. (In original: Podle starého vzoru: rekonstrukce malt, sgrafit a štuků.) (Praha: ITAM CAS, 2021).
36. Procházka, V. Chapel of St. Otilia in Vyškov. (In original. Kaple sv. Otilie ve Vyškově), Památky archeologické/Archaeological monuments XXXVI, pp. 258–266 (1930).
37. Babel, M. Badenian evaporite basin of the northern Carpathian Foredeep as a drawdown salina basin. *Acta Geol. Polonica* **54**, 313–337 (2004).
38. Bel-Anzué, P. & Elert, K. Changes in traditional building materials: the case of gypsum in Northern Spain. *Archaeol. Anthropol. Sci.* **13**, 177, https://doi.org/10.1007/s12520-021-01438-6 (2021).
39. Cardoso, I. P. & Pye, E. Gessoes in Portuguese Baroque gilding grounds, part 1: a study of historical documentary sources. *Stud. Conserv.* **62**, 185–209, https://doi.org/10.1080/00393630.2015.1130774 (2016).
40. Elert, K., Benavides-Reyes, C. & Cardell, C. Effect of animal glue on mineralogy, strength and weathering resistence of calcium sulfate-based composite materials. *Cem. Concr. Compos.* **96**, 274–283, https://doi.org/10.1016/j.cemconcomp.2018.12.005 (2019).
41. Oates, J. A. H. Lime and limestone. Chemistry and technology, production and uses. 1st ed., (Wiley-VCH, Weinheim, 1998), p. 455.
42. Caroselli, M. et al. Gypsum in Ticinese stucco artworks of the 16–17th century: Use, characterization, provenance and induced decay phenomena. *J. Archaeol. Sci. Rep*. **24**, 208–219. https://doi.org/10.1016/j.jasrep.2019.01.009 (2019).
43. Eastaugh, N., Walsh, V., Chaplin, T. & Siddall, R. Pigment Compendium: A Dictionary of Historical Pigments (1st ed.). https://doi.org/10.4324/9780080473765 (2004).

Acknowledgements

This research was carried out within the Erasmus+ project STUDEC—Stucco Decoration Across Europe, grant number 2022-1-CZ01KA220-HED-000085652. We thank Dr. Štěpánka Kučková and the Laboratory of Applied Proteomics of the University of Chemistry and Technology Prague for the analysis of the organic additives and our colleague, and Dr. Radek Ševčík from the Department of Materials Research of ITAM CAS for carrying out XRD analysis.

Author contributions

J.V.—main concept of the research, survey and sampling, analytical work, writing of the paper, proofreading. M.C.—survey and sampling, analytical work—microscopy, writing of the paper. S.S.P.—survey and sampling, analytical work—SEM EDS, analysis of coating layers, writing of the paper. P.K.—survey and sampling, analytical work—Optical microscopy, writing of

the paper, formatting and production. J.Z.—main concept of the research—art history, writing of the paper, proofreading. D.F.—analytical work—Thermal analysis, writing of the paper. K.K.—sample processing, analytical work—acid dissolution, formatting of the paper for production

Competing interests
The authors declare no competing interests.

Additional information
Correspondence and requests for materials should be addressed to Marta Caroselli.